High ON/OFF Ratio and Quantized Conductance in Resistive Switching of TiO_2 on Silicon

Chengqing Hu, *Student Member, IEEE*, Martin D. McDaniel, John G. Ekerdt, and Edward T. Yu, *Fellow, IEEE*

***Abstract*— TiO_2 has been investigated extensively as an active resistive switching (RS) material for resistive random access memory. In this letter, single-crystal anatase-TiO_2 thin films fabricated on silicon by atomic layer deposition are used to realize highly stable and clean bipolar RS behavior with a record high ON/OFF ratio ($\sim 10^7$) and low leakage current in the high-resistance state. The switching characteristics resemble those of electrochemical memories via formation and dissolution of conductive filaments (CFs) composed of oxygen vacancies, and small numbers of quantized channels are reproducibly observed in the low-resistance state, consistent with quantized conductance (QC) found in conventional electrolytic systems and indicating its potential for forming ultrathin CF amenable to device scaling. A detailed analysis of QC and contact resistance is presented. The emergence of QC is believed to be related to the single-crystal nature of the TiO_2 thin films.**

***Index Terms*— Conductive filament (CF), metal oxide, nonvolatile memory, quantized conductance (QC), resistive random access memory (RRAM), resistive switching (RS), titanium dioxide.**

I. INTRODUCTION

METAL-oxide resistive random access memory (RRAM) has been under intense investigation for next-generation nonvolatile memory owing to its high density, excellent scalability, low power consumption, fast switching speed, and compatibility with conventional complementary metal–oxide–semiconductor technology [1], [2]. Among the various metal oxides that have been found to exhibit resistive switching (RS) behavior, TiO_2 has enjoyed particular prominence for RRAM applications, memristors, reconfigurable analog integrated circuits, stateful implication logic, and neuromorphic computing [3]–[9].

Despite the extensive studies on TiO_2-based RRAM, the detailed mechanism driving its switching behavior remains controversial, and different models have been proposed to understand the underlying physics [3]–[6]. Nevertheless, it is widely accepted both theoretically [10], [11] and experimentally [4], [5], [12], [13] that formation and rupture of a localized conductive filament (CF) composed of oxygen vacancies is the crucial element in realizing RS in TiO_2. In this letter, we report the first demonstration of RS in single-crystal TiO_2 thin films, evidence consistent with quantized conductance (QC) of CF formed during RS in TiO_2, and a record high ON/OFF ratio for RS in this material system.

Manuscript received August 1, 2013; revised August 29, 2013; accepted September 11, 2013. Date of publication September 30, 2013; date of current version October 21, 2013. This work was supported in part by the National Science Foundation under Award DMR-1006725, in part by the Office of Naval Research under Grant 14-10-1-0489, and in part by the J. S. Swearingen Regents Chair in Engineering at The University of Texas at Austin. The review of this letter was arranged by Editor M. Jurczak.

C. Hu and E. T. Yu are with the Microelectronics Research Center and the Department of Electrical and Computer Engineering, The University of Texas at Austin, Austin, TX 78758 USA (e-mail: ety@ece.utexas.edu).

M. D. McDaniel and J. G. Ekerdt are with the Department of Chemical Engineering, The University of Texas at Austin, Austin, TX 78712 USA.

Color versions of one or more of the figures in this letter are available online at http://ieeexplore.ieee.org.

Digital Object Identifier 10.1109/LED.2013.2282154

II. EXPERIMENTAL DETAILS

Epitaxial single-crystal anatase TiO_2 thin films either 8- or 15-nm thick were grown by atomic layer deposition (ALD) on n+ Si (001) substrates ($\rho \sim 0.01\ \Omega$·cm) using a single-crystal strontium titanate (STO) buffer layer. Four unit cells of STO grown by molecular beam epitaxy serves as a template for ALD growth. For the 8-nm film, no annealing was performed; for the 15-nm film, an *in situ* vacuum anneal was performed at 250 °C for 1 h after the growth of the first 3-nm TiO_2, resulting in formation of oxygen vacancies and Ti^{3+} species while minimizing the formation of amorphous SiO_x at the STO-Si interface. More details regarding growth of the TiO_2/STO/Si heterostructures can be found in [14] and [15].

The 200-μm diameter circular top electrode (TE) contacts to the 8-nm (15 nm) TiO_2 were formed by photolithography, e-beam evaporation of 5-nm (8 nm) Ti/160-nm Au, and liftoff. A Ti/Au bottom electrode (BE) was deposited onto the bottom of the n+ Si substrate. The RS behavior of the films was measured in air at room temperature by an Agilent 4156A precision semiconductor parameter analyzer in current–voltage (I–V) sweep mode. The sweeping voltage V was applied to the TE with the BE grounded. A voltage sweep that turns the device from high-resistance state (HRS) to low-resistance state (LRS) is defined as a SET process, whereas the reverse process is defined as RESET. During the SET process, the compliance current I_{comp} was set between 10 μA and 1 mA to prevent hard breakdown in the TiO_2 films unless otherwise indicated.

III. RESULTS AND DISCUSSION

The X-ray diffraction spectrum [Fig. 1(a)], reflection high-energy electron diffraction images [Fig. 1(b)] of the as-deposited 8-nm TiO_2 film, and transmission electron microscope imaging of as-deposited anatase-TiO_2/STO/Si [14] identical to the 8-nm sample in this letter confirm the high quality of the interfaces and crystallinity of the films. The device structure along with crystal structures of the epitaxial stack for both 8- and 15-nm TiO_2 cells are shown in Fig. 1(c).

Fig. 2(a) shows a continuous series of 0 V $\rightarrow$ +1 V $\rightarrow$ 0 V voltage sweeps, with no I_{comp} set and no RESET applied

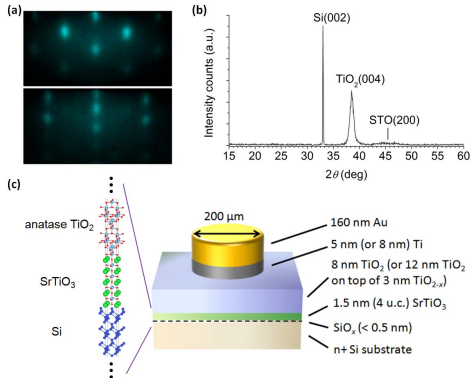

Fig. 1. (a) Reflection high-energy electron diffraction images obtained from as-deposited 8-nm-thick TiO_2 film on four-unit cell STO-buffered Si (001). The beam is aligned along the [110] (top image) and the [210] azimuth (bottom image). (b) X-ray diffraction spectrum of the as-deposited TiO_2/STO/Si sample. (c) Schematic diagram of the device structures and crystal structures of the involved epitaxial stack under investigation.

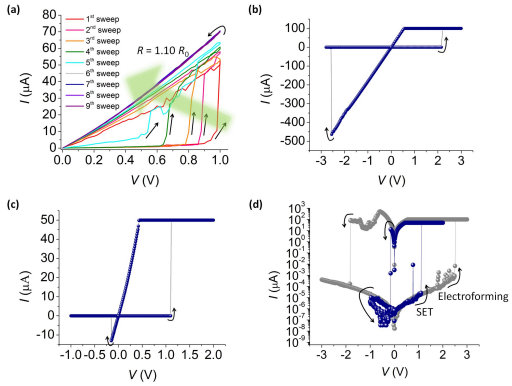

Fig. 2. (a) Series of consecutive voltage sweeps performed on a 15-nm TiO_2 device showing that the LRS was stabilized in the regime of QC. (b) Typical RS I–V characteristics of a 15-nm TiO_2 device with $I_{comp} = 100\ \mu$A. (c) Typical RS I–V characteristics of an 8-nm TiO_2 device with $I_{comp} = 50\ \mu$A. (d) Log I–V version of (c) showing a large ON/OFF ratio (blue) and an electroforming process with $I_{comp} = 100\ \mu$A on that device (grey).

between the consecutive sweeps, on a 15-nm TiO_2 device after applying a 0 V $\rightarrow$ +8 V $\rightarrow$ 0 V $\rightarrow$ −8 V $\rightarrow$ 0 V electroforming voltage sweep (with a forming threshold voltage of 2 V) on the pristine device without I_{comp}. Each of the first five sweeps was accompanied by a SET process with decreasing threshold voltage and slightly increasing ON-state conductance indicating formation of a weak CF. This structure is prone to disruption via self-accelerated diffusion of oxygen vacancies by Joule heating at the beginning of the following sweep [16], but prior studies have shown that CFs are stabilized by filling of electrons in the oxygen vacancies to increase cohesion among ostensibly positively charged vacancies [11] and the small capture section of electron-occupied oxygen vacancies to interstitial oxygen ions [17]. Linear I–V curves were observed for the subsequent sweeps, all with total resistance $R = 1.10\ R_0$, where $R_0 = h/(2e^2) \sim 12.9\ \text{k}\Omega$ is the intrinsic contact resistance of a single-mode ballistic conductor sandwiched between two conductive contacts [18]. This observation is suggestive of LRS conduction via a fully bridged and single quantized channel, whereas the stable behavior observed for the final four sweeps is consistent with reduction of the electric field across the TiO_2, and consequent suppression of oxygen vacancy motion upon formation of a conducting path stabilized against Joule heating. Fig. 2(b) shows typical RS I–V characteristics with I_{comp} set at 100 μA for a 15-nm TiO_2 device, for which $I_{comp} = 100\ \mu$A and the same voltage sweep range as shown in Fig. 2(b) were applied during the electroforming process (not shown). Due to the annealed 3-nm TiO_x bottom layer, the electroforming of the 15-nm TiO_2 devices occurs at the identical threshold voltage as that of a SET process under the same compliance current, further indicating the key role of oxygen vacancies in RS. In addition, RS occurs for the following sweeps when the device of Fig. 2(a) was operated in the same way as that in Fig. 2(b). Fig. 2(c) shows typical RS I–V characteristics with $I_{comp} = 50\ \mu$A for an 8-nm TiO_2 device, for which the corresponding log I–V and electroforming process ($I_{comp} = 100\ \mu$A) are shown in Fig. 2(d). The electroforming process for which $I_{comp} = 100\ \mu$A is applied occurs at the threshold voltage higher than the SET voltage, regardless of the I_{comp} applied for the SET process. All measured 8-nm TiO_2 devices show large ON/OFF ratios ($\sim 10^7$) and extremely low leakage in the HRS, consistent with the very small electron mobility in TiO_2 [19]; ON/OFF ratios of $\sim 10^5$ were found for the 15-nm TiO_2 devices (not shown). These ON/OFF ratios suggest possible applications in pulse-based multilevel nonvolatile memory [1], [2].

Evidence indicative of QC for LRS is seen for both the samples. Although the TiO_2 growth process minimizes the formation of SiO_x at the STO-Si interface, a SiO_x layer thinner than 0.5 nm is still expected [14]. This amorphous layer dominates the extrinsic contact resistance R_C since insertion of a Ti layer between Au and TiO_2 significantly lowers the Schottky barrier of the top contact [6], and the conduction band edges of TiO_2, STO, and Si are approximately aligned in the presence of oxygen vacancies [20]–[22]. Thus, the total measured LRS resistance, $R_{tot,LRS}$, can be expressed as

$$R_{tot,LRS} = R_C + R_0/n \tag{1}$$

where n denotes the number of modes for a ballistic conductor. For any particular device, R_C varies only slightly from measurement to measurement since STO acts as a barrier to drift and diffusion of oxygen vacancies from the TiO_2 at room temperature [23] and keeps the SiO_x layer relatively intact. Since R_C is unknown *a priori*, n cannot be determined directly from the measured $R_{tot,LRS}$. Furthermore, in successive instances of LRS for a particular device, n may vary slightly due to its sensitivity to the nanoscale structure of the channel. Thus, for each device we performed 10–20 measurements of $R_{tot,LRS}$ by cycling repeatedly through the device ON and OFF states as shown in Fig. 2(b) and (c). Each measured value of $R_{tot,LRS}$ can correspond to different combinations of R_C and n, subject to the constraints as follows: 1) $0 < R_C < R_{tot,LRS}$ and 2) large values of n are effectively indistinguishable since $R_{tot,LRS}$ approaches R_C for large n. For each measurement of $R_{tot,LRS}$, we compute all possible combinations (R_C, n) allowed by (1) with an (arbitrary) upper limit of $\sim$20 for n. Our results are not sensitive to the specific value of this upper limit. If N combinations are allowed, we assign each a weight of $1/N$ and compute the resulting statistical distribution for R_C,

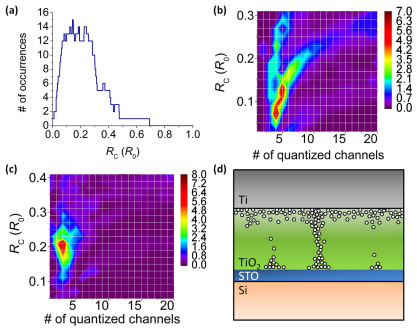

Fig. 3. (a) Number of occurrences of R_C out of the 17 SET–RESET sweeps with $I_{\text{comp}} = 100\ \mu$A for SET process performed on an 8-nm TiO_2 device as a function of contact resistance R_C. (b) Surface plot of number of occurrences versus R_C and number of quantized channels for the 17 sweeps in (a). (c) Surface plot similar to (b) for a 15-nm TiO_2 device over the 20 SET–RESET sweeps and $I_{\text{comp}} = 100\ \mu$A. (d) Schematic illustration of a LRS CF in TiO_2.

summed over all measurements for a particular device. Such a distribution for 17 measurements on one representative device with 8-nm TiO_2 is shown in Fig. 3(a) and implies that R_C is between $0.05R_0$ and $0.3R_0$. The corresponding distribution for n with R_C in this range is shown in Fig. 3(b). For $R_C \approx 0.1R_0$, this distribution is sharply peaked around $n = 4$–5, suggesting that a nanoscale QC channel with a small number of quantized modes is formed repeatedly and reproducibly. Fig. 3(c) shows the analogous distribution for a device with 15-nm TiO_2, for which we see $R_C \approx 0.2R_0$ and $n = 3$, indicative of repeated and reproducible formation of a QC channel in that device. For all the measured devices, the distribution is always peaked at $n = 2$–5, for both 8- and 15-nm TiO_2.

It should be noted that although metal oxides are not generally known as solid electrolytes, the high ON/OFF ratio, low electronic leakage in the HRS, and linear I–V characteristics in the LRS found here strongly resemble features of electrochemical metallization memories (as opposed to electronic or valence-change based) [1], suggesting that the CF bridges the whole film during SET and mostly dissolves during RESET. This is further corroborated by Fig. 2(a) and a detailed analysis of the HRS I–V characteristics of the devices (to be reported elsewhere). Electrolyticlike RS behavior has been associated with QC, as previously reported [24].

Our observations suggest that either a single or very small number of CFs is formed repeatedly and reproducibly in each device, as shown schematically in Fig. 3(d). We believe this to be related to the single-crystal nature of the TiO_2 film, in which fewer paths, compared with a polycrystalline film, may be available for CF nucleation. This reproducibility and the large ON/OFF ratios observed suggest that these materials may be promising for scaling of RRAM cells to nanoscale dimensions at which QC will be inevitable.

IV. Conclusion

We demonstrate repeatable and stable bipolar RS behavior in single-crystal TiO_2 thin films with a record high ON/OFF ratio and consistent with QC, suggesting future exploration of single-crystal TiO_2 as a candidate for RRAM cell scaling.

References

[1] R. Waser, R. Dittmann, G. Staikov, *et al.*, "Redox-based resistive switching memories—Nanoionic mechanisms, prospects, and challenges," *Adv. Mater.*, vol. 21, nos. 25–26, pp. 2632–2663, 2009.

[2] H.-S. P. Wong, H.-Y. Lee, S. Yu, *et al.*, "Metal–oxide RRAM," *Proc. IEEE*, vol. 100, no. 6, pp. 1951–1970, Jun. 2012.

[3] S. K. Kim, K. M. Kima, D. S. Jeonga, *et al.*, "Titanium dioxide thin films for next-generation memory devices," *J. Mater. Res.*, vol. 28, no. 3, pp. 313–325, Feb. 2013.

[4] B. J. Choi, D. S. Jeong, S. K. Kim, *et al.*, "Resistive switching mechanism of TiO_2 thin films grown by atomic-layer deposition," *J. Appl. Phys.*, vol. 98, no. 3, pp. 033715-1–033715-10, 2005.

[5] D. S. Jeong, H. Schroeder, U. Breuer, *et al.*, "Characteristic electroforming behavior in Pt/TiO_2/Pt resistive switching cells depending on atmosphere," *J. Appl. Phys.*, vol. 104, no. 12, pp. 123716-1–123716-8, 2008.

[6] J. J. Yang, M. D. Pickett, X. Li, *et al.*, "Memristive switching mechanism for metal/oxide/metal nanodevices," *Nature Nanotechnol.*, vol. 3, pp. 429–433, Jul. 2008.

[7] D. B. Strukov, G. S. Snider, D. R. Stewart, *et al.*, "The missing memristor found," *Nature*, vol. 453, pp. 80–83, May 2008.

[8] Y. V. Pershin and M. D. Ventra, "Practical approach to programmable analog circuits with memristors," *IEEE Trans. Circuits Syst. I, Reg. Papers*, vol. 57, no. 8, pp. 1857–1864, Aug. 2010.

[9] J. Borghetti, G. S. Snider, P. J. Kuekes, *et al.*, "'Memristive' switches enable 'stateful' logic operations via material implication," *Nature*, vol. 464, pp. 873–876, Apr. 2010.

[10] S.-G. Park, B. Magyari-Köpe, and Y. Nishi, "Impact of oxygen vacancy ordering on the formation of a conductive filament in TiO_2 for resistive switching memory," *IEEE Electron Device Lett.*, vol. 32, no. 2, pp. 197–199, Feb. 2011.

[11] K. Kamiya, M. Y. Yang, S.-G. Park, *et al.*, "ON-OFF switching mechanism of resistive–random–access–memories based on the formation and disruption of oxygen vacancy conducting channels," *Appl. Phys. Lett.*, vol. 100, no. 7, pp. 073502-1–073502-4, 2012.

[12] D.-H. Kwon, K. M. Kim, J. H. Jang, *et al.*, "Atomic structure of conducting nanofilaments in TiO_2 resistive switching memory," *Nature Nanotechnol.*, vol. 5, pp. 148–153, Jan. 2010.

[13] J. P. Strachan, M. D. Pickett, J. J. Yang, *et al.*, "Direct identification of the conducting channels in a functioning memristive device," *Adv. Mater.*, vol. 22, no. 32, pp. 3573–3577, 2010.

[14] M. D. McDaniel, A. Posadas, T. Q. Ngo, *et al.*, "Growth of epitaxial oxides on silicon using atomic layer deposition: Crystallization and annealing of TiO_2 on $SrTiO_3$-buffered Si(001)," *J. Vac. Sci. Technol. B*, vol. 30, no. 4, pp. 04E111-1–04E111-6, 2012.

[15] M. D. McDaniel, A. Posadas, T. Wang, *et al.*, "Growth and characterization of epitaxial anatase TiO_2(001) on $SrTiO_3$-buffered Si(001) using atomic layer deposition," *Thin Solid Films*, vol. 520, no. 21, pp. 6525–6530, 2012.

[16] D. Ielmini, F. Nardi, and C. Cagli, "Universal reset characteristics of unipolar and bipolar metal-oxide RRAM," *IEEE Trans. Electron Devices*, vol. 58, no. 10, pp. 3246–3253, Oct. 2011.

[17] B. Gao, B. Sun, H. Zhang, *et al.*, "Unified physical model of bipolar oxide-based resistive switching memory," *IEEE Electron Device Lett.*, vol. 30, no. 12, pp. 1326–1328, Dec. 2009.

[18] S. Datta, *Electronic Transport in Mesoscopic Systems*, 1st ed. Cambridge, U.K.: Cambridge Univ. Press, 2002, pp. 48–116.

[19] M. Katayama, S. Ikesaka, J. Kuwano, *et al.*, "High quality anatase TiO_2 film: Field-effect transistor based on anatase TiO_2," *Appl. Phys. Lett.*, vol. 92, no. 13, pp. 132107-1–132107-3, 2008.

[20] A. C. Tuan, T. C. Kaspar, T. Droubay, *et al.*, "Band offsets for the epitaxial TiO_2/$SrTiO_3$/Si(001) system," *Appl. Phys. Lett.*, vol. 83, no. 18, pp. 3734–3736, 2003.

[21] S. A. Chambers, T. Ohsawa, C. M. Wang, *et al.*, "Band offsets at the epitaxial anatase TiO_2/n-$SrTiO_3$(001) interface," *Surf. Sci.*, vol. 603, no. 5, pp. 771–780, 2009.

[22] H. Seo, A. B. Posadas, C. Mitra, *et al.*, "Band alignment and electronic structure of the anatase TiO_2/$SrTiO_3$(001) heterostructure integrated on Si(001)," *Phys. Rev. B*, vol. 86, no. 7, pp. 075301-1–075301-9, 2012.

[23] W. Jiang, M. Noman, Y. M. Lu, *et al.*, "Mobility of oxygen vacancy in $SrTiO_3$ and its implications for oxygen-migration-based resistance switching," *J. Appl. Phys.*, vol. 110, no. 3, pp. 034509-1–034509-8, 2011.

[24] K. Terabe, T. Hasegawa, T. Nakayama, *et al.*, "Quantized conductance atomic switch," *Nature*, vol. 433, pp. 47–50, Jan. 2005.